CHAPTER 4

MOTOR INSULATION SYSTEM AND TRANSIENT PRODUCED BY VARIABLE SPEED DRIVES

4.1 INTRODUCTION

Worldwide, various standards exist which specify various operating and constructional parameters of a motor. The two most widely used parameters are the National Electrical Manufacturers Association (NEMA) and the International Electro-technical Commission (IEC). Standards followed for manufacturing electric motors are from INDIAN STANDARD INSTITUTION.

NEMA

NEMA sets standards for a wide range of electrical products, including motors. NEMA is primarily associated with motors used in North America. The standards developed represent the general industry practices and are supported by manufacturers of electrical equipment. These standards can be found in the NEMA Standard Publication No. MG 1. Some large AC motors may not fall under NEMA standards. They are built to meet the requirements of a specific application. They are referred to as above NEMA motors.

IEC

IEC is a European-based organization that publishes and promotes worldwide, the mechanical and electrical standards for motors, among other things. In simple terms, it can be said that the IEC is the international counterpart of the NEMA. The IEC standards are associated with motors used in many countries. These standards can be found in the IEC 34-1-16. The motors which meet or exceed these standards are referred to as IEC motors.

The NEMA standards mainly specify four design types for AC induction motors – Design A, B, C and D. Their typical torque-speed curves are shown in Figure 18.

Design A has normal starting torque (typically 150-170% of rated) and relatively high starting current. The breakdown torque is the highest of all the NEMA types. It can handle heavy overloads for a short duration. The slip is <= 5%. A typical application is the powering of injection molding machines.

Design B is the most common type of AC induction motor sold. It has a normal starting torque, similar to Design A, but offers low starting current. The locked rotor torque is good enough to start many loads encountered in the industrial applications. The slip is <= 5%. The motor efficiency and full-load PF are comparatively high, contributing to the popularity of the design. The typical applications include pumps, fans and machine tools.

Design C has high starting torque (greater than the previous two designs, say 200%), useful for driving heavy breakaway loads like conveyors, crushers, stirring machines, agitators, reciprocating pumps, compressors, etc. These motors are intended for operation near full speed without great overloads. The starting current is low. The slip is <= 5%.

Design D has high starting torque (higher than all the NEMA motor types). The starting current and full-load speed are low. The high slip values (5-13%) make this motor suitable for applications with changing loads and subsequent sharp changes in the motor speed, such as in machinery with energy storage flywheels, punch presses, shears, elevators, extractors, winches, hoists, oil-well pumping, wire-drawing machines, etc. The speed regulation is poor, making the design suitable only for punch presses, cranes, elevators and oil well pumps. This motor type is usually considered a "special order" item.

Recently, NEMA has added one more design – **Design E** – in its standard for the induction motor. Design E is similar to Design B, but has a higher efficiency, high starting currents and lower full-load running currents. The torque characteristics of Design E are similar to IEC metric motors of similar power parameters.

The IEC Torque-Speed Design Ratings practically mirror those of NEMA. The IEC Design N motors are similar to NEMA Design B motors, the most common motors for industrial applications. The IEC Design H motors are nearly identical to NEMA Design C motors.

There is no specific IEC equivalent to the NEMA Design D motor. The IEC Duty Cycle Ratings are different from those of NEMA's. Where NEMA usually specifies continuous, intermittent or special duty (typically expressed in minutes), the IEC uses nine different duty cycle designations (IEC 34 -1).

Normally motor design as per different standards is meant for operation on sinusoidal supply

Prior to the introduction of insulated gate bipolar transistor (IGBT) switching devices, the main issue motor designers were concerned with in mating a motor to an adjustable speed drive (ASD) was the increase in temperature rise from the harmonic losses the ASD introduced [34].

With the introduction of the IGBT ASD, a second issue has become as important as the thermal issue-insulation integrity. When long cable lengths are used between the motor and the ASD, transmission line theory explains that when

the motor surge impedance is high compared to the cable characteristic impedance, the effect is voltage doubling (test show even higher than doubling) on leading edge of the voltage pulse at the motor [35]. On pulse width modulation (PWM) ASDS, thousands of pulses per second are applied to the motor. The National Electrical Manufacturers Association (NEMA) recognized that these pulses could damage the motor insulation and has written into their standard NEMA MG1-31 that motor designed for use on ASDs must be capable of operation in the presence of 1600 V peak amplitude pulses with a rise time of 0.1 microsecond or greater [36]. NEMA standard MG1-30 also defines the insulation capability of the standard motors used on drives to a much lower number- 1000 V peak with a 2 microsecond rise time [37].

Voltage rise time is a very important parameter in determining motor insulation system integrity. It determines voltage amplitude at the motor (in conjunction with the cable length between the motor and the ASD) and voltage distribution in the individual motor coils.

It should be noted that voltage doubling did occur on ASDs prior to the introduction of IGBT switches. However, the previous technology switches (GTOS and bipolar junction transistors) had longer rise times resulting in voltage doubling occurring with longer cable lengths and more even voltage distribution in the motor windings. The net effect of these is that ASDs with IGBT switches have more severely stressed motor insulation.

4.2 MOTOR WINDINGS

To understand the various ways motors are built to handle the higher voltage amplitude and voltage distribution differences an ASD introduces, it is necessary to understand the type of the coils of the winding. There are two type of coils used in motor winding; (1) Form Coil and (2) random wound coil.

Motor built for medium voltage applications are rated for the system voltages to which they are applied. At medium voltages, motors are typically built with form coil windings. Form coil windings have insulated rectangular wire, and are carefully taped or wrapped and varnished to eliminate the presence of air so that partial discharge between wires is avoided. (Partial discharge is defined as the ionization of air leading to an electrical breakdown in a void of any geometry within insulation subjected to an electric field). The nature of the construction assures that the turns are in sequential order. Therefore, Turn 1 would only touch Turn 2, Turn 2 would only touch Turns 1 and 3, etc. with this careful turn placement, the voltage between adjacent wires is limited to the turn to turn voltage.

Conversely, on low voltage systems - 600 V and below – motors are usually built with what is known in the industry as random windings. Random wound motors

are wound with multiple strands of round magnet wire and are often wound on tooling to specific shape, then inserted into the stator slots. During this wind/insert process, the adjacent wires could in the worst case have the first and the last turn touching (hence the term random winding). If the first and last turns are in contact within a coil, adjacent turn voltage can be full coil voltage, not sequential turn voltage. Additionally, on some types of random coil windings, the end turns of adjacent coils are not separated, so in the end turns, turns in adjacent coils can touch, resulting in adjacent wire voltage exceeding coil voltage.

Random windings are often vacuum pressure impregnated (VPI), dip, or flood varnished. This is done in an attempt to eliminate all air pockets between wires, replacing them with varnish. The numerous crossovers and wire interfaces combined with the round wire geometry make it virtually impossible to eliminate all the air pockets. As stated above, these little air pockets make partial discharges possible if an adequate voltage to start the partial discharge is presented.

As can be seen, the two big differences between the forms coil and random windings are:

- Adjacent wire voltage can be higher in the random winding, and
- Random windings are more likely to have air pockets between wires. (Air is a necessary ingredient for partial discharges.)

4.3 RISE TIME AND PEAK VOLTAGE CONCERNS

The voltage is evenly distributed across all the windings in slowly changing voltage signals like 50 Hz sine wave power. But with short rise times a disproportionate portion of the voltage is distributed across the first coil – sometimes reaching in excess of 75% of the total line to line voltage across the coil [38].

Since a large part of the total line to line voltage can be across the first coil, since the line to line voltage at the motor can be as much as twice the voltage at the ASD terminals (as explain by transmission line theory), and since the first and last turns of a coil can in worst case be touching (the first turn of the first coil can even be touching a turn in the second coil in the end turn- as explained above), it will be noted that the presence of the IGBT PWM ASD can greatly increase the voltage between adjacent wires in a random wound motor.

These higher voltages present between adjacent wires in a random-wound motor can be high enough that partial discharge occurs. Standard random wound machines were not designed for operation in partial discharge environment.

Reiterating, the factors that bring adjacent turn voltages high enough so that partial discharge may occur include:

- The short rise time of an IGBT drives causes uneven voltage distribution putting high voltages on the first coil.
- With the long cable lengths, the voltage may exceed twice what it would be if the ASD were next to the motor terminals, and
- The use of random winding on low voltage motors creates a possibility of full coil voltage between adjacent wires.

L. Manz [39] has reported that average life for the insulation is 10^8 cycle when voltage level is 600 V. The life of the insulation decreases with increase in voltage level and becomes 10^7 cycles when voltage increases to 4500 V. the sharp decrease in life with present magnet wire operating in partial discharge; it is a requirement that motors be operated below the starting voltage for partial discharge for the long life expected from today's motors. Some of the premature failures seen when operating standard motors with IGBT PWM ASDs are due to partial discharge. These motor can fail within months (even weeks) of installation.

Adjustable speed drives fed from modern frequency converters with voltage source inverters (VSI) are operated in a wide range of traction and industrial applications. The converters that employ modern power electronic devices provide more flexible motor operation, low torque ripple, improved system efficiency and many other benefits. Unfortunately some unintended disturbances accompany operation of these drives. Well-known transient over voltages stress insulation system of fed motor and dramatically decrease motor lifetime. Recently, it is recorded in practice tremendous over voltages with peaks that significantly exceed twice dc bus voltage level. Such surges cause very fast motor insulation breakdown. Familiarity with motor overvoltage theory, understanding of generation causes and knowledge of factors that influence these surges are necessary for design of whole drive system and for development of diagnostic methods. Investigation of high frequency transient effects requires exact model of the drive system. A lot of very interesting papers have reported on motor over voltages [40] - [48], however, this effect is still not sufficiently described. Literature is especially lacking on general theory of surges that lead to overshoots significantly exceeding twice dc bus voltage.

Zdenek Peroutka [49] has presented simulation and experiments results which have been performed for both laboratory set-ups (4kW/400V/50Hz). As an illustrative example, tests were performed on main drive of light rail vehicle recently developed in `koda Electric. His experimental set-up was consisting of frequency converter with PWM voltage source inverter and induction motor that is connected by power cable to the converter. Output transformer was placed at inverter output. The application of step-up transformer is typical for example for drives used in oil exploitation or in mining industry. Protective devices could be connected on either converter or motor terminals. A lot of very sophisticated models of frequency converter with voltage source inverter have been published in literature [50]. For investigation of motor transient over voltages, frequency converter's model can

often be simplified with sufficient accuracy. Voltage source inverter can be replaced by controlled voltage sources that generate trapezoidal pulses. The model may be completed by resistance and stray inductance in order to get better accuracy of dc link output impedance. However, such simplified model is not useful in all cases. More complex analysis (e.g. design of some filters) requires considering properties of dc bus circuit and input rectifier.

Power cable models can be divided into two basic groups:

1) Models with lumped parameters and 2) models with distributed parameters.

In first case, the cable is replaced by finite number of equivalent networks with lumped parameters in cascade connection. The problem is how to choose the number of networks? It is suggested to estimate the number of networks (*n*) based on crucial cable length (*l*c). Crucial cable length legibly define border between system with lumped and distributed parameters. This border is of course not an exact line between these systems. Crucial length is expressed as:

$$l_c = \frac{v * t_{rise}}{2} = \frac{c * t_{rise}}{2 * \sqrt{\varepsilon_r}} \quad (4.1)$$

Where t_{rise} is rise time of inverter's voltage pulses, v is wave velocity, c is speed of light t_{rise} and ε_r is relative permittivity of cable insulation material. It is well-known that *v* is closed to half of speed of light, because ε_r of common cables is approximately 4 ÷ 5. The number of equivalent networks for cable of length *l* is given by:

$$n = \frac{l}{l_c} = \frac{2l}{v * t_{rise}} = \frac{2l\sqrt{\varepsilon_r}}{c * t_{rise}} \quad (4.2)$$

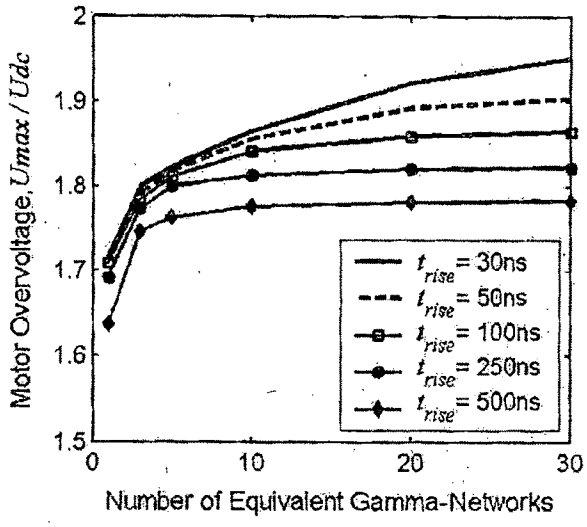

Impact of number of cable's equivalent networks on investigated characteristics at the motor terminals; cable length l = 50 m, U_{dc} is dc bus voltage
Figure 4.1

From Fig. 4.1 is evident, how peak voltage at the motor terminals (and of course other important characteristics as oscillation frequency, rise time of the voltage at the motor terminals) is approaching exact value with increasing number of equivalent networks. From a number of performed simulations, it is possible to conclude that 10 gamma networks get sufficient accuracy in range of typical cable lengths (up to 100m) and rise times (down to tens nanoseconds).
Number of distributed models have already been published- distortion less line model [51]; multi-node model [47] and especially very interesting model [52]. In his research Zdene k Peroutka [49] has proposed general transmission line model. [53, 54]. This model is directly based on continue mathematical model of transmission line – telegraph equations that represents system of partial differential equations. The results are shown in figure 4.2.

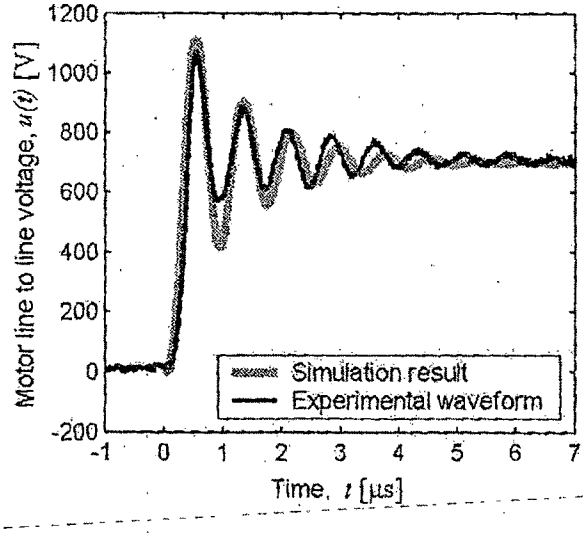

Detail of line to line voltage waveform at motor terminals, f_c = 2 KHz, f_{out} = 60 Hz
Figure 4.2

The design of the ac stator winding insulation must take into consideration both the steady-state operating voltages and the voltage transients (surges) caused by the factors such as lightning strikes and switching phenomena. Both types of over voltages stress the ground insulation and, if the surge is steep enough, also over-stress the turn insulation. Steep-fronted surges with magnitudes as high as 4.5 per unit (pu) and rise times of 0.1- 0.2 microsecond are possible during normal breaker operation, where one pu is the crest of the rated line-to-ground voltage or

$$1\,pu = \sqrt{\frac{2}{3}} * rated\ line\ voltage$$

Surge voltages of 6 pu and higher are not unknown.
Next to bearing failure, turn insulation failure is probably the most common failure mode in ac motors. Since this type of failure also usually leads to ground wall insulation failure, a turn insulation failure has been mistaken as a ground wall insulation failure by motor users in the past. Because of the wide uses of vacuum switching devices, and a large numbers of studies undertaken, awareness of turn insulation performance and potential problems has, in recent years, been heightened in the minds of motor users.

Turn insulation failures typically occur in the stator end-winding and usually at the first bend from the straight portion where the coil exit the slot, or at the nose of the coil. This is so because bending and pulling operations during coil manufacturing place additional strain on insulation at these locations causing it to lose some dielectric strength.

Turn insulation failures can be due to crack in the insulating materials, deficiencies in insulation design, irregularities in manufacturing, or inadequate quality control. In operation, they can also be caused by voltage surges that are higher or more frequent than the specified capability, poor preventive maintenance practices, normal deterioration of insulation dielectric strength with time , or mechanical rubbing of one insulated part with another due to coil movements as might be the case during motor starting, speed switching, and motor vibration.

4.4 SURGES

The standards make a distinction between impulses and surges. An impulse[34] is an intentionally applied a periodic transient voltage which usually rises rapidly to a peak value and then falls more slowly to zero, whereas a surge refers to transients occurring in electrical equipment of networks in service.

There are two kinds of surges or transient over voltages; those originated by lightning strikes and those caused by switching phenomena. The standards again makes a distinction [55] between switching and lighting surges on the bases of the duration of the front or the rise time from zero to peak value. Surges, with fronts of up to 20 μs are defined as lighting surges, and those with longer fronts are defined as switching surges.

The actual shape- the rise and decay times and the amplitude-can vary enormously. Therefore, it is necessary to define these surges by relatively simple means for simulation and testing purposes. A standard lightening surges is defined as one having a virtual front time of 1.2 μs and a virtual time to half value of 50 μs. A steep-fronted surge is one with a rise time of 0.1-0.5 μs and a virtual time to half value of around 5 μs (Figure 4.3).

A steep-fronted surge with a rise of 0.2 μs appears entirely across the first or line end coil of the winding. Further, its distribution in the coil is not quite linear. This results in voltage stresses across the turn insulation that is much higher than the steady-state values. It is for this reason that most turn insulation failures occur in the line coils.

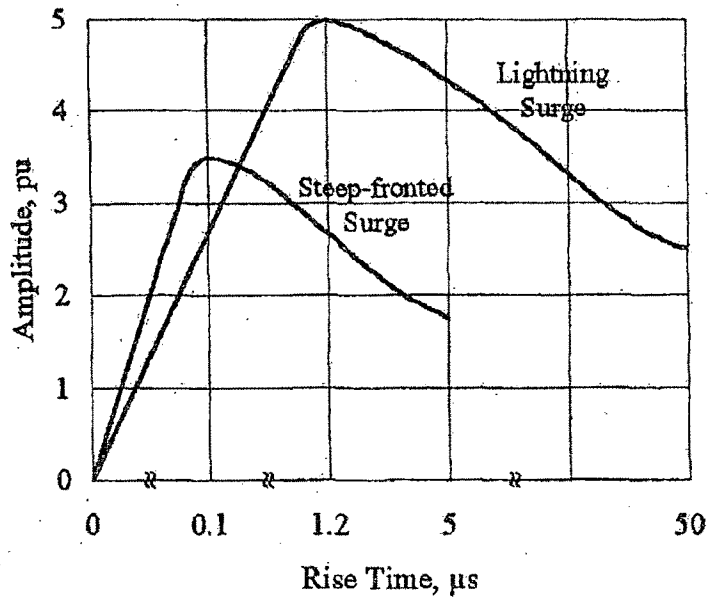

Lighting and steep-fronted surges
Figure 4.3

4.5 THE SURGE ENVIRONMENT

The availability and use of new and improved materials and devices and the desire to produce cost-effective competitive products has resulted in greater exposure of the motor to high amplitude, steeper–fronted surges. Because of their reliability, compact size, low maintenance needs, and longer life IGBT drives are most widely used. However they produce repetitive, high amplitude, steep-fronted surges. The use of low loss a cable between the drive and the motor does not increase the surge front or lower its amplitude.

IGBT drives are used to achieve operational economies. The increase in motor power densities due to improved technology, economic and competitive considerations, and the need to reduced losses and improve efficiencies has resulted in motors that are less conservatively designed than they used to be. They do not use dedicated turn insulation when not required by the design. The strand insulation is now designed to function as h turn insulation also.

Thus, it has become increasingly important to understand the surge phenomena, its causes, the system parameters that affect their amplitudes and rise time, and the manner in which these surges distribute themselves in the windings so

as to permit adequate design of the turn insulation and/or of motor surge protection.

4.6 FACTORS AFFECTING SURGE AMPLITUDE AND RISE TIMES

The amplitude and rise time of the surge appearing at the motor terminals depends on the operating voltage, the system design, characteristics of the devices in the system, and indeed the design of motor itself. The following factors are important in this regards:

1) Transient event taking place:

a) Rate of normal pulses:

b) Motor starting:

c) Aborted starts:

d) Switching locked rotor insures current;

e) Winding being switched:

f) Bus transfer.

2) Motor:

a) Capacitance and surge impedance (and hence motor size);

b) Parallel circuits.

3) Cable connecting the motor to the breaker and its characteristics:

a) Type single phase, triplexed or, belted);

b) Cable insulation;

i) XLPE, EPR (low loss);

ii) PVC, PILC (HIGHER LOSS);

C) Cable length;

d) Whether shielded or unshielded;

e) Whether the shield is grounded, and if so, where.

4) Power devices

a) IGBT

b) MOSFETs

c) Power Transistor

d) GTO

5) Other loads connected to the bus.

6) The device between drive and motor which is making connection:

a) Air-magnetic break;

b) Vacuum breaker;

c) Maximum chopping current, contactor material and design.

4.7 STEEP FRONTED SWITCHING SURGES

4.7.1 BREAKER TYPES

Circuit breakers can be classified as vacuum, SF6, air-magnetic, and minimum oil. Air-magnetic breakers have been popular in the US. Vacuum breakers are used universally and because of economic considerations are now used in a large number of installations.

Voltage transients are produced by circuit breakers during contact opening as well as contact closing. Air-magnetic breakers produce a fast rise time surge during closing only, whereas the vacuum breaker produces steep-fronted surges during opening as well as closing. Also, switching in vacuum produces multiple surges during closing (prestrike) and opening (reignitions). Thus, for a single event of opening or closing, the vacuum breaker produces multiple surges and, therefore, stresses turn insulation more than other switching devices. Further, multiple reignition causes each successive surge to be at a level higher than the previous one. Larger numbers of prestrike are possible at 13.2 KV than 4 KV

4.7.2 SURGE GENERATION

All three contacts in a circuit breaker do not close or open simultaneously due to minor differences I the contact travel times. Some times more than one load is feed from a single bus. Figure 2 is such a motor cable breaker bus system. If Z_c is the motor cable surge impedance and all cables are connected to the bus are identical, V_i is the instantaneous value of the surge launched into the motor cable when the first contact closes or prestrike, V is the instantaneous line to ground system voltage, *n* is the number of cables connected to the same bus, then it can be shown [56, 57] that approximately

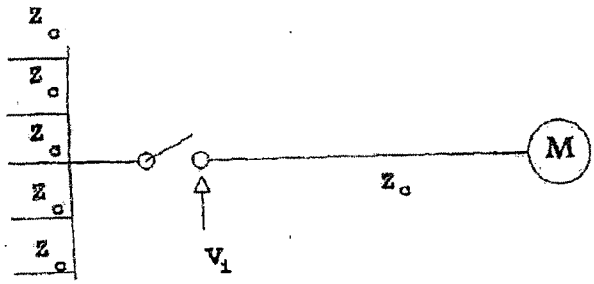

Figure 4.4 Typical cable-motor system

$$V_i = V\left[\frac{Z_c}{Z_c + \frac{Z_c}{n}}\right] = V\left[\frac{n}{n+1}\right] \text{\_\_\_\_[4.3]}$$

When this surge arrives at the motor terminals (a point of discontinuity since the surge impedance undergoes a change here), wave reflection back into the cable, and refraction into the motor winding takes place. If Z_m is the motor surge impedance, the amplitude V_m of the surge at the junction that propagates into the motor winding is

$$V_m = V_i\left[\frac{2Z_m}{Z_m + Z_c}\right] \text{\_\_\_\_[4.4]}$$

If

$$Z_m \gg Z_c \; then$$

$$V_m \gg 2V_i$$

i.e. under some extreme system conditions, the surge amplitude at the motor terminals can be almost twice the level of the surge injected into the cable at the circuit breaker. This surge will cause the motor cable system to oscillate at its natural frequency and the magnitude of the peak voltage across the second and third contacts of the breaker can be as high as $2.5V_i$. If at this time a prestrike occurs, a $2.5V_i$ surge will be applied to the motor cable and the doubling effect could result in a surge of almost $5V_i$ at the motor terminals [56]

$$V_m = 2.5 * V\left[\frac{n}{n+1}\right]\left[\frac{2Z_m}{Z_m + Z_c}\right] \text{ ——[4.5]}$$

The wave front duration of this surge is

$$\frac{3\left[\frac{n}{n+1}\right]L_b}{Z_c} \text{ —[4.6]}$$

Where Z_c is the equivalent inductance of the bus to which the motor is connected [57].

4.7.3 CABLES

The type of motor-to-breaker cable used and the manner in which it is grounded has an effect on the amplitude and rise time of the surge arriving at the motor terminals [58]. The lower the loss in the cable, the lower is the attenuation of the surge; the higher the loss, the higher will be the attenuation. Typically, if the cable is long, the attenuation is larger. However, with modern low loss cables (for example, EPR) practically no attenuation of the surge takes place, irrespective of the length of the cable.

The surge impedance of the cables is different for shielded and unshielded cables. Unshielded cables have relatively high surge impedance. The use of such cables will reduce the magnitude of the surge arriving at the motor terminals, whereas shielded cables will tend to increase the magnitude.

Even in shielded cables, the location of the ground affects the surge profile at the motor. If ground at the motor end, shielded cables reduce the amplitude of the surge. On the other hand, the rise time increases if it is ground at the drive end.

The propagation velocity of surges through an insulated feeder cable is about 150 m/ μs. If the motor surge impedance is larger than cable surge impedance, the cable is longer than 15 m and the surge wave front is o.1 μs, voltage doubling is possible. The minimum cable length for this phenomenon is 30 m. for a surge wave front of o.2 μs.

4.8 MOTOR DESIGN EFFECTS

The inter-turn voltage is a function of the number of series turns per coil and phase. It can thus be reduced by decreasing the number of parallel circuits and correspondingly increasing the number of series turns in the winding.

If the stator winding is not an all-series winding but has more than one parallel circuit in each phase, then, depending on the size and design, the terminations of all parallel circuits may either be brought out into the lead box, or

paralleling bars or rings used inside the machine and only two leads per phase brought out. The latter design introduces an inductance between the motor terminal and the lead end coils. This has an effect of increasing the rise time of the surge and limiting the inter-turn voltage.

4.9 SURGE DISTRIBUTION IN THE WINDING

When the steep-fronted surge arrives at the motor terminals, its propagation through the winding and the dielectric stresses it imposes on the turn insulation are a function of its rise time. Many studies have been made [59, 60], and models developed to study the surge distribution in the winding. In general, these studies are based on the treatment of the winding as a single conductor or multi-conductor transmission line and represent it as a set of series and parallel lumped or distributed parameters consisting of capacitances, inductances, and conductances for each conductor (half turn), turn or coil. These studies indicate that for steep-fronted surges:

1) The distribution of the surge across the winding is non-uniform and almost the entire surge appears across the line end coil;

2) The surge distribution in the coil is not uniform, especially when the rise time is 0.3 μs or less.

3) The distribution depends on the thickness of the ground wall and turn insulation, and the shape, size, and length of the slot and end-winding portions of the coils.

Sensitivity studies [59], [61] and [63] also indicate that:

1) The steepness of the surge front (i.e. the rise time of the surge) and the number of turns per coil are the major factors in determining the severity of the dielectric stress on the insulation;

2) Inter-turn surge voltage could be as high as 130% of the average value for a surge with a rise of 0.1 μs and 125% of the average value for a surge with a rise of 0.2 μs this ratios are essentially independent of the machine voltage (and, hence, insulation design) and of the coil size;

3) Insulation thickness, shape of the coil, size of the coil (its width and length), and relative length of stator core and overhang portion of the coil have a minor impact on the turn insulation dielectric stress severity.

4.10 STANDARDS

The standards that deal with surges are the following.

1) IEEE Standard 522-1992: IEEE guide for testing turn-to turn insulation on form-wound stator coils for alternating current rotating machines [63]

2) IEEE Standard 792-1987: IEEE Trial-Use Recommended Practice for the Evaluation of the Impulse voltage Capability of the Insulation Systems for AC Electrical Machinery Employing Form wound Stator coils [64].

3) NEMA MG1-1993: Motors and generators [65].

4) IEC 34-15, 1990: Rotating Electrical machines, Part 15: Impulse Voltage withstand Levels of Rotating ac Machines with form-wound coils [66].

5) Draft International Standard 2 (co) 557: Revision of IEC 34-15: 1990 [67].

All of these standards apply to form wound ac windings only, there are no standards for performance or test for motors with random winding, such as the NEMA medium motors in size 500 HP and less at voltages 600 V and below.

NEMA MG1 specifies surge capabilities as well as test methods. It establishes 2 pu at a rise time of 0.1- 0.2 μs and 4.5 pu at a rise time of 1.2 μs or longer as the standard surge withstand capability. A capability of 3.5 pu at a rise time of 0.1- 0.2 μs and 5 pu at a rise time of 1.2 μs or longer are offered as options when agreed upon between the vendor and user. The methods and instrumentation are as per IEEE Standard 522.

4.11 CAUSES OF TURN INSULATION FAILURES

Turn insulation can fail for a number of reasons, not all of them within control. These could be design, quality, and site condition related:

1) The dielectric stress due to the surge exceeding the capacity of the turn insulation;

2) A much larger number of surges per unit time than was foreseen when the motor was specified and designed;

3) Insulation degradation over a time under the influence of normal dielectric and thermal stresses, moisture, vibration, and contaminations;

4) Turn insulation erosion due to corona if voids exist in locations next to the turn insulation, resulting in partial discharge; this is likely to happen at voltage greater than 6000 V and with voids larger than 0.05 mm in diameter;

5) Turn insulation erosion over time if due to high vibration, repeated start, and speed switching, the insulation work loose and relative movement becomes possible between individual turns in a coil;

6) Inadequate or absent routine and preventive maintenance of the motor;

7) A much more hostile surge environment than was originally envisioned.

Therefore, following points are to be considered while designing the inter-turn insulation.

1. Knowledge of the surge environment in which the motor is to operate is necessary in determining the surge capability requirements of the motor.
2. Although system studies can be made to determine the worst case surge that might impinge on the motor winding, the monitoring of surges at a number of sites on an industry-wide basis over a period of time is desirable to develop a better feel for surge requirements.
3. The surge capability specified for a motor should be based on application requirements, not simply on any particular standard. This is so because actual requirements might be the same, less, or greater than what the standards require.
4. Higher than necessary level of surge capability and specified dedicated turn insulation are not quite "free". Both the size (first cost) and the efficiency (operating expenses) are adversely affected. Dedicated surge protection equipment for the motor should be considered as a factor in the economic analysis for motor selection.
5. The application of dedicated turn insulation is no guarantee of freedom from failure. If the surge amplitude, rise time, and frequency of surges per unit time are higher than those specified, dedicated turn insulation can also fail.
6. In critical applications, irrespective of the level and type of turn insulation specified, the use of dedicated surge protection should be considered.
7. A large number of motors are functioning satisfactorily with a surge capability of 2 pu. It is not necessary to make a global switch to higher surge capability windings, since in many applications the surge environment is not very hostile.
8. A need exists for a standard definition for surges withstand capability of stator winding turn insulation. This definition should address not only the amplitude and rise times, but also the number of such surges that the insulation must be capable of withstanding.

H.A. Toliyat [68] has presented a method of estimating the voltage distribution among the windings of an inverter fed random wound induction motor supplied through feeder cable. For investigation he has used inverter-cable-motor model and the transient analysis is performed using ATP (Alternative Transient Program) package to estimate the voltage distribution among the motor winding. In his work he has shown the method of

(1) estimating the high frequency parameters of the feeder cable and the motor, (2) estimating the voltage distribution among the turns and coils of the motor windings with and without feeder cable and (3) developing a comprehensive high frequency model for the cable and the motor in ATP which can be used for analyzing the various phenomena like terminal voltage doubling, effect of filters at the motor terminals, evaluating the voltage transients with different types and configurations of the cables, etc.

In order to form an equivalent circuit for the system, the distributed parameters of the cable and the motor need to be used because of the high frequency content of the sharp rising wave fronts. For example, if the rise-time of the wave front is 0.2 μs, then the parameters should be evaluated at 5 MHz and so on. The high frequency parameters to be used in the distributed equivalent circuit for the motor include the resistance of each turn, self-inductance of each turn, mutual inductances between the turns, turn-to-ground capacitance and turn-to-turn capacitances. Since the magnetic behavior of the steel at MHz range frequencies will be entirely different from that at power frequencies. He reported that the characteristic impedance of commonly used cable is around 75 ohm [69] while the characteristic impedance of the motor will be much higher and varies over a wide range of values depending on the power rating of the motor.

For computing the turn resistances and inductances, the eddy current solver available in the package is used. A single slot model is used to obtain the parameters in which one stator slot with the along with their insulation are modeled. In the present case, there are 54 turns within a slot. In order to simplify the model, only a two dimensional model for the slot is used for computing the field. This assumes a fixed relative positioning of the conductors with in the slot. For obtaining the impedance of all the turns in the slot, the eddy current solver was used. Setting up the eddy current analysis includes defining material properties, setting up excitation, defining boundary conditions, etc. when eddy current analysis is used; the package automatically defines each conductor as a current source. The only boundary condition used is balloon boundary condition in which a surface far away from the slot model is set to zero magnetic vector potential. The eddy current field solver calculates the eddy currents by solving for A and $\emptyset$ in the field equation:

$$\nabla_x \frac{1}{\mu_r}(\nabla_x * A) = (\sigma + j\omega\varepsilon_r)(-Aj\omega - \nabla\emptyset)$$

Where, A is he magnetic vector potential, $\emptyset$ is the electric scalar potential, μ_r is the relative magnetic permeability, ω is the angular frequency at which all quantities are oscillating, σ is the conductivity, ε_r is the relative permittivity.

The Maxwell 2D simulator computes the impedance matrix in two steps. First, it solves for the inductances matrix associated with the model. Second, it solves for the matrix resistance and then forms the impedance matrix. The frequency for which the analysis has to be done can be defined while formulating the problem. The simulator generates an eddy-current field solution for each conductor in the model. The first turn is set to 1 A current in the first solution with all other turns current set to zero current. In the second solution, only the second turn is set to 1 A with the other turns set to zero current. After each solution, the inductance and resistance are

computed from the magnetic energy stored and the associated ohmic loss respectively. After each field solution, the solver calculates the self inductance of the conductor which was assigned 1 A current during the analysis. Also, the mutual inductances of the conductor with all the other conductors are computed. Similarly, the resistance terms are also computed after each field solution. The final output of the eddy current analysis is a 54 x 54 impedance matrix. After each solution, the inductances and resistances are computed using the following relations:

$$L = \frac{4U_{AV}}{I_p^2} \; and \; R = \frac{2P}{I_p^2}$$

Where,
U_{AV}= the energy stored in magnetic field in Joules,
P = ohmic loss in watts,
I_p= peak value of current in ampere

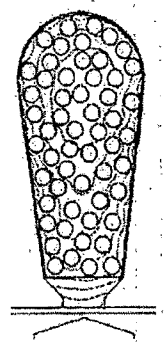

Flux distribution in the slot obtained with eddy current analysis
Figure 4.5

The flux plot obtained from the eddy current analysis shows an interesting influence of the high frequency behavior of the machine. The flux plot obtained from the eddy current analysis is shown in figure 4.5. The flux plot shows that the flux lines are confined to the slot portion itself and the flux lines do not penetrate the steel laminations because of high frequency effects. Also, there is no flux passing through the air gap to the rotor. The impedance matrix also shows that the different turns have different impedances depending on their relative positioning within the slot.

The capacitance matrix is also obtained in a similar way. For computing the capacitance matrix, electrostatic field analysis is performed with the same geometry. During electrostatic analysis, each conductor is defined as a voltage source and assigned 1 V potential with all the other conductors set to 0V. The electrostatic field simulator computes the static field arising from potential differences and charge distributions. After each field simulation, the capacitance values associated with the conductor which was assigned 1V are competed, which includes turn-to-ground and the turn-to-turn capacitances between the turn being excited and all the other turns.

Unlike the impedance calculation procedure, the capacitance calculation need not be carried out at high frequency since the capacitance values are not influenced much by the frequency of excitation. The electrostatic field simulator basically computes static fields arising from potential differences and charge distributions. The field simulator solves for the electric potential, $\emptyset(x, y)$, in the field equation derived from Gauss's law and is given by

$$\nabla \cdot (\varepsilon_r \varepsilon_0 \nabla \emptyset(x, y)) = -\rho$$

ε_0= permittivity of free space.
ρ= charge density

To compute the capacitance matrix, the Maxwell 2D field simulator performs a sequence of electrostatic field simulations. For an n-conductor system, n-field simulations are performed. The capacitance between conductor's j and k is therefore:

$$c = 2U_{jk}$$

U_{jk}= energy in the electric field associated with flux lines that connect charges on conductor k to those on conductor k.

The equivalent circuit parameters of the turns depend highly on the relative positioning within the slot. For example, turns which are adjacent to each other will have higher mutual coupling (both turn-to-turn mutual inductance and capacitance) compared to turns which are far apart. Similarly turns which are adjacent o the slot wall have higher capacitance-to-ground compared to the slot the ones interior to the slot. Figure 4.6 show the variation of self-inductance of individual turns with distance along the width of a slot and figure 4.7 shows the corresponding turn-to-ground capacitance values.

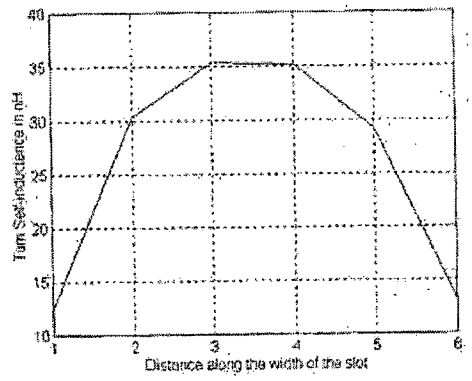

Variation of self-inductance of individual turns with distance along the width of the slot (scale: X-axis 1 div. = 1 mm)
Figure 4.6

Figure 4.6 show that the turns which are adjacent to the slot wall have lower self-inductance values compared to the ones which are interior to the slot because of the vicinity of ground.

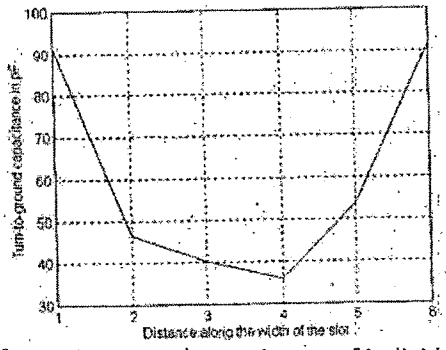

Variation of turns to ground capacitance of individual turns with distance along the width of the slot (scale: X-axis 1 div. = 1 mm)

Figure 4.7

The relative positioning of the turns affects their mutual inductance and capacitance values also. For example, two turns which are adjacent to each other have typical mutual inductance values of 20 nH and turns which are far apart have negligible mutual coupling. Similarly, turns which are adjacent to each other have typical capacitance values around 22 pF and turns which are far apart have negligible mutual capacitance. Another observation is that the turns which are located around the periphery of the slot wall have almost identical self-inductance values and so are the turns which are interior to the slot.

The parameters of the feeder cable at frequencies will also be significantly different from its power frequency values. In the present work, the cable constant routine available in ATP package is used for obtaining the high frequency parameters. ATP is the personal computer version of the Electro Magnetic Transient Program (EMTP). First, the geometry and material data of the three phase cable is defined in an input file in a format specified by the ATP users' manual [70]. The type of cable used for connecting the inverter and the motor in the present case is type A as designated in the ATP user manual, viz, a system of coaxial cable without any enclosing pipe. After defining the geometry and physical data, the frequency for which parameters need to be computed is specified. With this input data file, the "Cable Constants" routine is used to compute the parameters at the frequency specified. The parameters of he cable are also computed for a frequency of 5 MHz corresponding to a rise-time of 0.2 μS.

To obtain the voltage distribution among the motor windings, an equivalent circuit model for the inverter-cable-motor system is created in ATPDRAW. The details of the equivalent circuits used are explained in the following subsections.

The output of the voltage source PWM inverter will have a train of wave fronts with very sharp rise-times. The transient voltage pattern among the winding during each PM wave front remains the same throughout the cycle (unless the width of any pulse is so small that before he transients due to rising edge dies down, the falling edge arrives and vice versa. [38]. There will also be several wave fronts occurring in each fundamental cycle. Hence in order to understand the transients

during a wave front, it is sufficient to model only one front applied across any two lines of the motor [68]. This simplifies the complexity of the model. In order to model a typical wave front, a RAMP type source is used in ATPDRAW. In ATPDRAW the amplitude, rise-time, starting and duration of the pulse can all be defined. In the present model, only one ramp source is used and applied across phases A & B with phase C open.

Cable can be modeled either as a lumped parameter pi-circuit or as distributed parameter circuit components. A third alternative is to approximate the distributed nature of the parameters by using several cascaded lumped parameter pi-sections. There is also a more advanced model which can account for changes in the parameters with frequency, however this not considered here due to the rather limited range of frequencies of interest. The main disadvantage of using the lumped pi-section model is that large numbers of sections need to be modeled since the wave lengths corresponding to MHz range frequencies will be very small. To avoid this problem, a distributed parameter model is used in ATP.

From the high frequency parameters obtained from the finite element analysis, a distributed equivalent circuit for the motor is formed. The motor being analyzed in the present case has 54 turns per coil; there are 6 coils per phase pole, two groups of 3 coils being connected in parallel. Ideally, it would be desirable to model each turn within a slot with its distributed parameters and also its mutual impedances with other turn within the slot. However, considering the number of turns per slot, it is not practical to model all the turns with their distributed parameters. However, it is a well known fact that the first few turns of the line end coil get subjected to maximum voltage stress during each wave front [71]. Hence , in the present work, only the first few turns of the line end coil are represented by their distributed parameters with all the other turns in the line-end coil and also the other coils modeled by their lumped parameters; phases A and B are modeled the way explained, phase C is modeled by its lumped parameters.

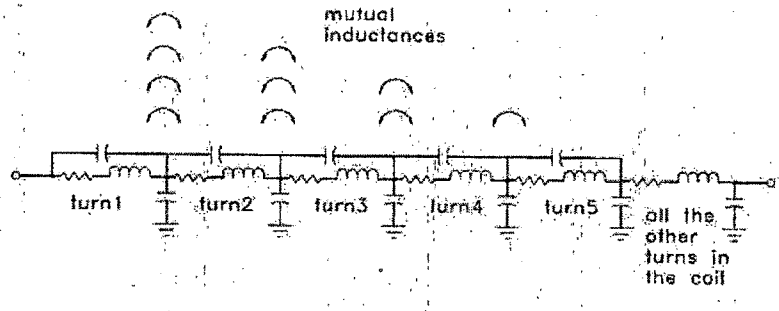

Partially distributed equivalent circuit of the line-end coil

Figure 4.8

Finite element analysis gives the per unit length values of the parameters of the turns modeled in the slot. Hence while forming the equivalent circuit; these values are multiplied by the mean length of turns which takes care of the end-turn portions of the turns. The equivalent circuit of the line-end coil described in this section is shown in figure 4.8.

To form the equivalent circuit for the whole system, first the ramp type source is inserted. One end of the source is grounded and the other end of the source is connected to one of the three phases in the cable distributed parameters. The output of the cable is connected to the motor equivalent circuit described earlier. This completes the generation of the equivalent circuit for the system. Once the equivalent circuit of the inverter-cable-motor system is developed in ATPDRAW, the type of analysis to be done, duration of analysis, and the time step for simulation are all defined after which ATP simulation performed.

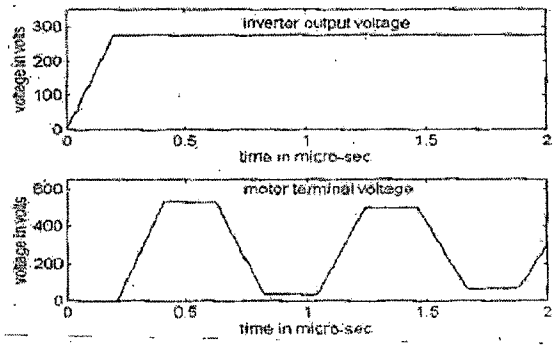

Simulated inverter output voltage and motor terminal voltage with100 foot long cable

Figure 4.9

For studying the terminal voltage transients only the feeder cable is modeled with distributed parameters as described earlier. The motor is represented by its lamped parameter model with impedance equal to its characteristic impedance. The characteristic impedance of the motors depends on their power rating and typical values are listed in [69]. In a present case, a resistance value of 1500 ohm is used to represent the motor. The main idea of this simulation is to study the terminal voltage transients in detail. As described earlier, the ATP file for the entire system model is created only once. When different cable lengths are to be simulated, the

corresponding entry in the ATP file is changed. Figure 4.9 shows the simulated terminal voltage transient along with the input PWM wave front of a cable length of 100 feet.

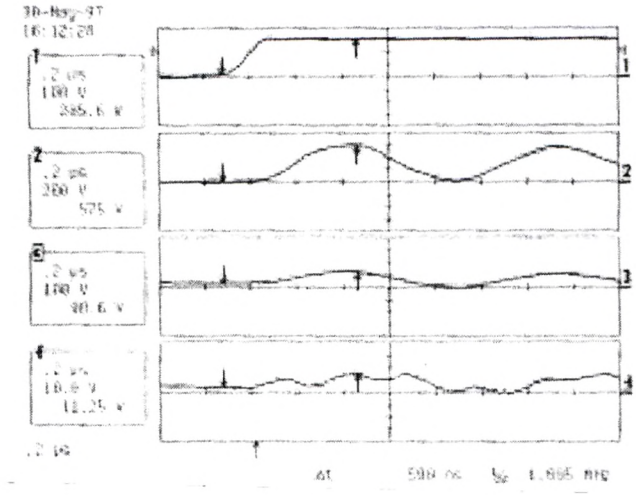

Experimental results of a PWM Induction motor drive with 100 foot long cable between the inverter and the motor. Trace 1: Inverter output voltage, Trace 2: Motor terminal voltage, Trace 3: Line end voltage, Trace 4: Turn 1 Voltage.
Figure 4.10

Figure 4.10 shows the measured waveforms of the inverter output voltage, motor terminal voltage, line-end coil voltage and turn 1 voltage when the motor is connected to the inverter through 100 feet cable. From the simulated and experimental results, it can be seen that the voltage takes some time to travel from the inverter output to the motor terminals which depends on the cable length. Comparing the amplitude and the frequency of oscillation of the motor terminal voltage, it can be seen that the simulated and experimental results match well.

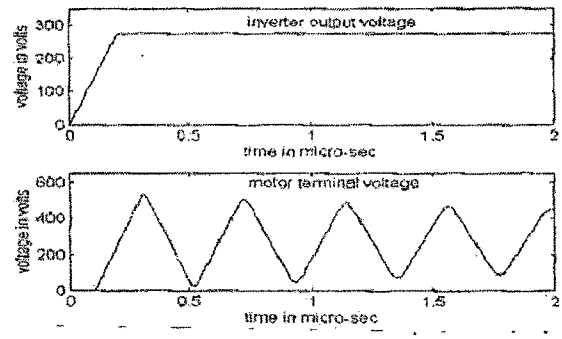

Simulated inverter output voltage and motor terminal voltage with 50 foot long cable

Figure 4.11

Figure 4.11 shows the simulated voltage wave forms with 50 feet long cable, comparing figures 4.9 and 4.11, it can be seen that the frequency of oscillation of the motor terminal voltage increases with reduction in cable length. This is because of the fact that voltage wave has to travel longer with increase in cable length while the velocity of propagation remains the same. Figure 4.12 and 4.13 show the simulated and measured inverter output voltage along with the motor terminal voltage when a 10 feet long cable is used. Though the cable length is not very long, some amount of oscillation and over voltage can be seen at the motor terminals. In this case also, good agreement between simulation and experimental results can be seen by comparing figures 4.12 and 4.13.

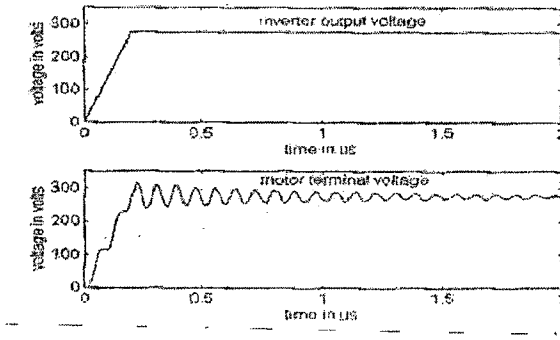

Simulated inverter output voltage and motor terminal voltage with 10 foot long cable

Figure 4.12

In the second simulation, the motor winding is modeled along with 10 feet cable and the wave front. The main idea is to study the voltage distribution among the windings when the motor is connected to the inverter through a 10 feet long cable. Figure 4.14 shows the line-end coil voltage when rise-time of the wave front is 0.2 μS.

In this simulation, both the feeder cable and the motor are represented by their distributed parameters. This simulation is performed to study the effect of voltage doubling on the voltage distribution among the windings. Figure 4.15 shows the voltage drop across the line end coil with 100 foot cable used to connect the motor and the inverter. The rise-time of the wave front is 0.2 μS. The measured line-end coil voltage with 100 foot cable is also shown in Figure 6. While the amplitude of the simulated and measured line-end coil voltages match well, the frequency of oscillations do not quite match well. This is mainly due to the approximate equivalent circuit model used for the motor windings which basically may not represent the actual time constants involved in the transients. As mentioned earlier, it would be desirable to represent all the turns within a given slot by its distributed parameters which would truly represent the high frequency circuit.

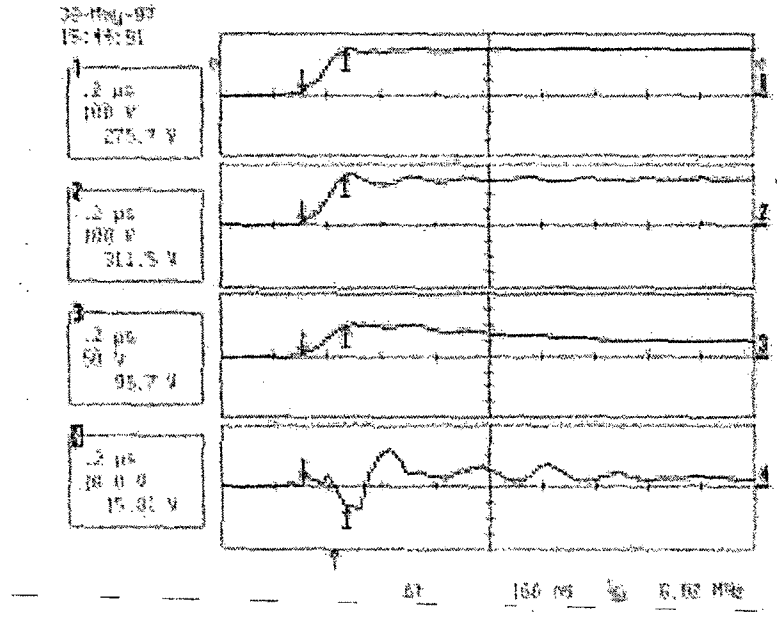

Experimental results of a PWM Induction motor drive with 10 foot long cable between the inverter and the motor. Trace 1: Inverter output voltage, Trace 2: Motor terminal voltage, Trace 3: Line end voltage, Trace 4: Turn 1 Voltage.

Figure 4.13

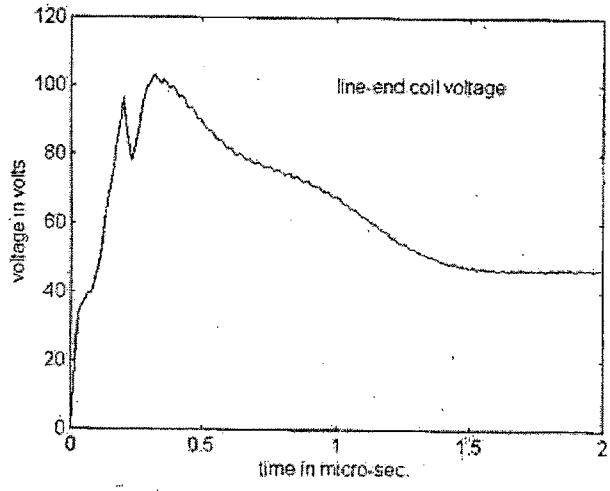

Line end coil voltage with 10 foot long cable

Figure 4.14

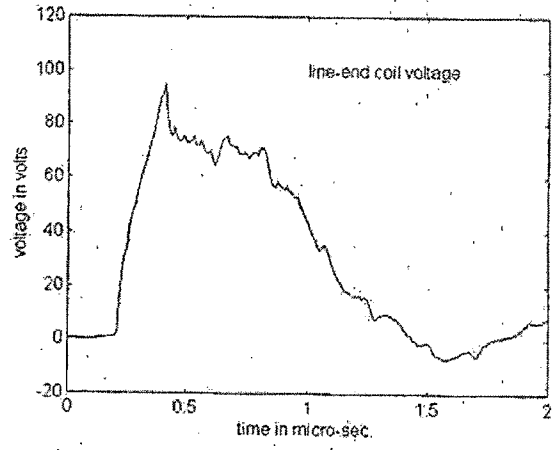

Line end coil voltage with 100 foot long cable and 0.2 μs rise time

Figure 4.15

One important observation made based on simulation and experimental results is that the peak value of the transient voltage across the line-end coil does not vary appreciably when the feeder cable is introduced, through there is voltage doubling at the motor terminals. In fact, the peak value of the line-end coil voltage slightly reduces when the feeder cable is used. It is an interesting result because, the insulation of the motor winding has to be designed based on this.

In random wound machines, the placement of the individual turns within a slot will be quite random in nature and there is a possibility that the first and the last turns of the same coil be placed adjacent to each other. In this case, the two turns are separated only by the thin insulation layers of the two turns. During a wave front, it is shown that a considerable portion of the line voltage is dropped across the line end coil and hence this might result in insulation break down. The main concern while using a long feeder cable is that the voltage stress on the line-end coil might be worse because of the terminal voltage doubling. However, the simulation and experimental results obtained in the present work do not show any such additional stress.